JOURNAL OF THERMOPHYSICS AND HEAT TRANSFER
Vol. 12, No. 4, October–December 1998

Inverse Estimation of Mix-Typed Boundary Conditions in Heat Conduction Problems

Ching-yu Yang*
National Kaohsiung Institute of Technology, Kaohsiung City 807, Taiwan, Republic of China

A sequential method is proposed to estimate various types of boundary conditions in the field of the inverse heat conduction. An inverse solution is deduced from the proposed method that is based on a numerical approach and the concept of future time. Special features about the proposed method is that no preselected functional form for the unknown function is necessary and no sensitivity analysis is needed in the algorithm. Furthermore, the mix-typed boundary conditions can be estimated in the proposed method. Two examples are used to demonstrate the characteristics of the proposed method. The results show that the proposed method is an accurate, robust, and efficient method to determine the boundary condition in the inverse heat conduction problems.

Nomenclature

$[A]$ = heat matrix
$[B]$ = transient matrix
$[C]$ = $(1/\Delta t)[K]^{-1}[B]$
$[D]$ = inverse matrix of $[K]$
E_k = $\sum_{l=0}^{k} e_l$
e = intermediate variable
h = convection heat transfer coefficient
$[K]$ = $[A] + (1/\Delta t)[B]$
q_n = heat flux
q_0 = value of temperature on Γ_q
$\{R\}$ = boundary vector
$\{R^c\}$ = vector of the unknown convection boundary
$\{R^q\}$ = vector of the unknown heat flux boundary
$\{R^T\}$ = vector of the unknown temperature boundary
$\{R^0\}$ = vector of the known boundary condition
r = number of the future time
T = temperature
$\{T\}$ = temperature vector
$\{\dot{T}\}$ = derivative of the temperature vector, $\{dT/dt\}$
T_b = value of temperature on Γ_T
T_f = value of temperature at which convection occurs
t = temporal coordinate
$\lfloor u^i \rfloor$ = unit row vector with a unit at i component
$\{u^*\}$ = unit column vectors with a unit at ( ) th component
V = general spatial domain
x, y = spatial coordinate
Y = measured temperature
α, β, γ, e = intermediate variables
Γ_c = boundary on which convection condition is prescribed
Γ_q = boundary on which heat flux condition is prescribed
Γ_T = boundary on which temperature condition is prescribed
λ = random number
Δt = increment of temporal domain
$\boldsymbol{\theta}$ = vector from previous state and the present known boundary
ρC = heat capacity per unit volume
σ = standard deviation of measurement error
ϕ^{c,i_c^j} = unknown convection condition at i_c^jth grid
ϕ^{q,i_q^j} = unknown heat flux condition at i_q^jth grid
ϕ^{T,i_T^j} = unknown temperature condition at i_T^jth grid
$\boldsymbol{\Phi}$ = vector from ϕ^{T,i_T^j}, ϕ^{q,i_q^j}, and ϕ^{c,i_c^j}
$\boldsymbol{\Omega}$ = sensitivity matrix
[ ] = matrix
{ } = column vector
⌊ ⌋ = row vector

Subscripts

i, j, k, l, m, n = indices
n_c = number of unknown grids of convection boundary
n_p = number of grids at spatial coordinate
n_q = number of unknown grids of heat flux boundary
n_T = number of unknown grids of temperature boundary
p = number of spatial measurement

Superscripts

exact = exact temperature
i, l, n = indices
i_c^j = grid number of the estimated convection temperature
i_q^j = grid number of the estimated flux function
i_T^j = grid number of the estimated temperature function
meas = measured temperature

Introduction

INVERSE heat conduction problems have been widely applied in many design and manufacturing problems, particularly when the direct measurements of the surface conditions are not possible, such as the measurement of the heat flux or temperature at the inner surface of a heated pipe, at the inside of a combustion chamber, at the outer surface of a re-entry vehicle, or at the tool-work interface of a machine cutting. Through the inverse technique the unknown boundary conditions can be deduced indirectly from the temperature measurements at different locations within the medium.

The inverse problem is ill posed, which means that one of the conditions on existence, uniqueness, and continuity of the

Received Nov. 3, 1997; revision received April 3, 1998; accepted for publication April 6, 1998.

*Professor, Department of Mold and Die Engineering. E-mail: cyyang@diemaking.de.nkit.edu.tw.

solution with respect to the measured data is not satisfied.[1] The uniqueness and existence of the inverse solution have been shown by Cannon[2] and Yang,[3] respectively. However, the inverse solution is often unstable even if the measured data have slight variations in the experimental measurements. Two important methods have been used to improve the stability of the estimation. One is the regularization method[4] and the other is the concept of future time.[5] The regularization function penalizes large variations in the unknown quantities by adding a term to the nonlinear least-squares error function. The concept of future time makes assumptions about the behavior of the experimental data at future time steps, which is added to the measurement in the nonlinear least-squares formulation. The analysis and application on the regularization method and on the concept of future time have been discussed.[5-12] Other methods used to solve the inverse problems based on the nonlinear least-squares formulation include the iterative regularization method,[7] the sequential regularization method,[5] dynamic programming,[13] the mollification method,[14] the adjoint equation approach coupled to the conjugate gradient method,[15] the Newton method,[16] and genetic algorithms.[17]

As previously mentioned, most of the methods adopt the nonlinear least-squares formulation in solving the inverse problem. When the value of the unknown boundary condition is assumed, this method executes a direct analysis to construct a residual function, i.e., the error function, from the sum of the squares of difference between the experimental measurements and the calculated responses of the system. Therefore, the iterative analysis is necessary to calculate the intermediate value for the construction of the error function. A nonlinear optimization process is needed as well to search for an improved vector for the unknown boundary. There are a few drawbacks in the preceding approaches. One is that the iterative process in the computation cannot be avoided and the other is that the inverse problem can only be solved in a nonlinear domain.

To solve the preceding problems, two whole domain methods, the reverse matrix method and the symbolic method, have been developed.[18,19] The features of the methods are that the computation in the inverse analysis process can be done only once and the problem can be solved in a linear domain. However, there are still problems in the preceding methods. In the process of the reverse matrix approach, the inversion of the heat matrix needs to be evaluated. This heat matrix is a square matrix with a size that is the product of the discretized interval in each coordinate. The size of the square matrix usually grows to be fairly large, particularly when it is a multidimensional problem. Even when the number of the discretized temporal steps is moderately small, the dimension of the heat matrix is still quite large. For example, when there are 11 mesh intervals along with each spatial coordinate and 100 mesh intervals along with the temporal coordinate in an inverse problem, the dimension of the heat matrix of a plate is 12,100. Therefore, the time spent in computation would be lengthy and the process would become inefficient. To resolve the problem, a symbolic approach has been adopted so that the inversion of the heat matrix can be avoided and the computation in the process can be done iteratively. However, in the process of the symbolic computation, there are still some side effects. One is that the growing size of the memory allocation is unpredictable and the other is that the efficiency of the computing process is not satisfactory.[20] Therefore, it is necessary to develop an efficient inverse algorithm to solve the preceding inverse problems.

In this paper a sequential method combined with the concept of the future time is proposed to solve problems that exist in the reverse matrix method and the symbolic approach. A numerical method can estimate various types of boundary conditions sequentially without the sensitivity analysis. In the proposed method, a closed-form is derived from a numerical model to explicitly represent the unknown boundary conditions. In the process of the derivation, a finite element difference method,[21,22] combined with the concept of future time,[5] is used to derive the result. The boundary condition is then determined step by step along with the temporal coordinate. Only the linear case is considered in this research. It means that there are no temperature-dependent coefficients in the heat equation or in the boundary conditions. The present analysis can be utilized to associate linearized equations in the nonlinear problems.

This paper contains five sections. In the first section, the current development of the inverse technique in the inverse heat conduction problems is introduced and the features of the proposed method are stated. In the second section, the characteristics of the inverse problem are delineated and the process of the proposed method is illustrated. In the third section, a computational algorithm of the method is proposed to be implemented in the computer. In the fourth section, two examples are employed to demonstrate the use of the proposed method; a discussion of the analyzed results is also presented in this section. In the fifth section, the overall contribution and possible applications of this research to the field of the inverse heat conduction problems are concluded.

Proposed Sequential Method to Estimate Boundary Conditions

Problem Statement

The inverse problem is to find one part of the boundary conditions in a two-dimensional body while the temperature measurements at the other part are given. Consider a two-dimensional body that is subjected to the following three boundary types (see Fig. 1): 1) The specified temperature $T = T_b$ on Γ_T, 2) the specified heat flux $q_n = q_0$ on Γ_q, and 3) the specified convection $q_n = h(T - T_f)$ on Γ_c. The interior of the body is denoted as V, and the boundary is denoted as $\Gamma = \Gamma_T \cup \Gamma_q \cup \Gamma_c$. Furthermore, q_n is the heat flux normal to the boundary. The sign convention adopted here for specifying q_0 is that $q_0 > 0$ if heat is flowing out of the body, whereas $q_0 < 0$ if heat is following into the body. The transient heat conduction problem is governed by the following equations:

$$\frac{\partial}{\partial x}\left(k\frac{\partial T}{\partial x}\right) + \frac{\partial}{\partial y}\left(k\frac{\partial T}{\partial y}\right) = \rho C\frac{\partial T}{\partial t}, \qquad (x_i, y_i) \in V \quad (1)$$

$$T(x_i, y_i, t) = T_b(x_i, y_i, t), \qquad (x_i, y_i) \in \Gamma_T \quad (2)$$

$$q_n(x_i, y_i, t) = q_0(x_i, y_i, t), \qquad (x_i, y_i) \in \Gamma_q \quad (3)$$

$$q_n(x_i, y_i, t) = h[T(x_i, y_i, t) - T_f(t)], \qquad (x_i, y_i) \in \Gamma_c \quad (4)$$

$$T(x_i, y_i, 0) = T_0(x_i, y_i), \qquad (x_i, y_i) \in \Gamma \cup V \quad (5)$$

where T represents the temperature field $T(x_i, y_i, t)$. k is the thermal conductivity, and ρC is the heat capacity per unit volume.

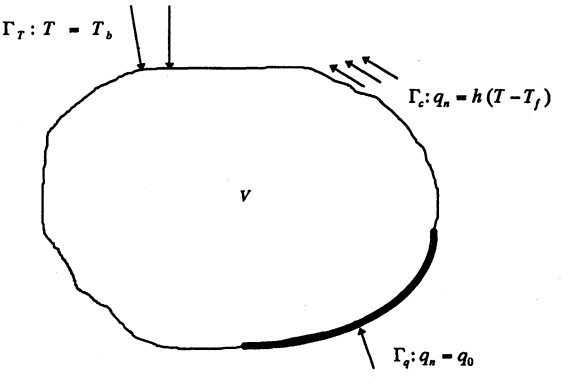

Fig. 1 Two-dimensional body with various types of boundary conditions.

The inverse problem is to estimate the unknown boundary conditions when the temperature field is measured at the known boundary. In the paper of Hsu et al.[23] it was mentioned that it is difficult to have an algorithm with the ability to estimate the heat flux and the surface temperature through the same technique in the multidimensional inverse heat conduction problem. However, the proposed method cannot only estimate the different types of boundary conditions separately, but it can also estimate various types of boundary conditions simultaneously.

Method to Determine the Boundary Conditions

In this section a numerical formulation is used to represent Eqs. (1–5) where the boundary condition is expressed as a vector form. The temperature distribution can be represented as the function of the boundary conditions, and then, the concept of future time is included in the proposed method. Finally, the inverse solution can be represented as a matrix equation.

The proposed method uses a finite element method with a linear triangular element to discretize the spatial coordinate. By the conventional finite element procedure with n_p grids at $t = t_j$ (Ref. 15), Eqs. (1–5) can be converted to the following discrete form:

$$[B]\{\dot{T}_j\} = \{R_j\} - [A]\{T_j\} \tag{6}$$

where $[A]$ is the heat matrix of the problem with n_p dimensions, $[B]$ is the transient matrix of the problem with n_p dimensions, $\{R_j\}$ is the boundary vector with n_p components, $\{T_j\}$ is the temperature vector with n_p components, and $\{\dot{T}_j\} = (\mathrm{d}/\mathrm{d}t)\{T_j\} = \{\mathrm{d}T_j/\mathrm{d}t\}$.

Next, we consider our finite element expression for $\{\dot{T}_j\}$ as a backward difference at time t_j. Therefore, we have

$$\{\dot{T}_j\} = (1/\Delta t)\{T_j\} - (1/\Delta t)\{T_{j-1}\} \tag{7}$$

Here Δt is the increment of the temporal coordinate.

By substituting Eq. (7) into Eq. (6), we have the following differential equation:

$$[K]\{T_j\} = (1/\Delta t)[B]\{T_{j-1}\} + \{R_j\} \tag{8}$$

where $[K] = [A] + (1/\Delta t)[B]$, $\{R_j\} = \{R_j^0\} + \{R_j^T\} + \{R_j^q\} + \{R_j^c\}$, $\{R_j^0\}$ is the vector of the known boundary condition, $\{R_j^T\}$ is the vector of the unknown temperature boundary, $\{R_j^q\}$ is the vector of the unknown heat flux boundary, and $\{R_j^c\}$ is the vector of the unknown convection boundary.

When $t = t_j$, the temperature distribution $\{T_j\}$ can be derived from Eq. (8) as follows:

$$\begin{aligned}\{T_j\} &= (1/\Delta t)[K]^{-1}[B]\{T_{j-1}\} + [K]^{-1}\{R_j\} \\ &= [C]\{T_{j-1}\} + [D]\{R_j\}\end{aligned} \tag{9}$$

where $[C] = (1/\Delta t)[K]^{-1}[B]$ and $[D] = [K]^{-1}$.

Similarly, the temperature distribution at $t = t_m, t_{m+1}, \ldots, t_{m+r-1}$ can be represented as follows:

$$\{T_m\} = [C]\{T_{m-1}\} + [D]\{R_m\}$$

$$\begin{aligned}\{T_{m+1}\} &= [C]\{T_m\} + [D]\{R_{m+1}\} \\ &= [C]^2\{T_{m-1}\} + [C][D]\{R_m\} + [D]\{R_{m+1}\}\end{aligned} \tag{10a}$$

$$\begin{aligned}\{\boldsymbol{T}_{m+r-1}\} &= [C]\{T_{m+r-2}\} + [D]\{R_{m+r-1}\} \\ &= [C]^r\{\boldsymbol{T}_{m-1}\} + [C]^{r-1}[D]\{R_m\} + [C]^{r-2}[D]\{R_{m+1}\} \\ &\quad + \cdots + [C][D]\{R_{m+r-2}\} + [D]\{R_{m+r-1}\}\end{aligned} \tag{10b}$$

Therefore, we have the temperature vector at $(m + n)$ temporal grid

$$\begin{aligned}\{T_{m+n}\} &= [C]^{n+1}\{T_{m-1}\} + \sum_{l=0}^{n}[C]^l[D]\{R_{m+n-l}\} \\ &= [C]^{n+1}\{T_{m-1}\} + \sum_{l=0}^{n}[C]^l[D]\{R_{m+n-l}^0\} \\ &\quad + \sum_{l=0}^{n}[C]^l[D](\{R_{m+n-l}^T\} \\ &\quad + \{R_{m+n-l}^q\} + \{R_{m+n-l}^c\})\end{aligned} \tag{11}$$

where n is an integer and $n = 0, 1, 2, \ldots, r - 1$.

After a unit row vector $\lfloor u^i \rfloor$ multiplies to both sides of Eq. (11), the temperature at i-spatial grid can be calculated as

$$\begin{aligned}T_{m+n}^i &= \lfloor u^i \rfloor[C]^{n+1}\{T_{m-1}\} + \sum_{l=0}^{n}\lfloor u^i \rfloor[C]^l[D]\{R_{m+n-l}\} \\ &= \lfloor u^i \rfloor[C]^{n+1}\{T_{m-1}\} + \sum_{l=0}^{n}\lfloor u^i \rfloor[C]^l[D]\{R_{m+n-l}^0\} \\ &\quad + \sum_{l=0}^{n}\lfloor u^i \rfloor[C]^l[D]\{R_{m+n-l}^T\} + \sum_{l=0}^{n}\lfloor u^i \rfloor[C]^l[D]\{R_{m+n-l}^q\} \\ &\quad + \sum_{l=0}^{n}\lfloor u^i \rfloor[C]^l[D]\{R_{m+n-l}^c\} \\ &= \lfloor u^i \rfloor[C]^{n+1}\{T_{m-1}\} + \sum_{l=0}^{n}\lfloor u^i \rfloor[C]^l[D]\{R_{m+n-l}^0\} \\ &\quad + \sum_{l=0}^{n}\sum_{j=1}^{n_T}\lfloor u^i \rfloor[C]^l[D]\{u^{i_T^j}\}\phi_{m+n-l}^{T,i_T^j} \\ &\quad + \sum_{l=0}^{n}\sum_{j=1}^{n_q}\lfloor u^i \rfloor[C]^l[D]\{u^{i_q^j}\}\phi_{m+n-l}^{q,i_q^j} \\ &\quad + \sum_{l=0}^{n}\sum_{j=1}^{n_c}\lfloor u^i \rfloor[C]^l[D]\{u^{i_c^j}\}\phi_{m+n-l}^{c,i_c^j}\end{aligned} \tag{12}$$

where

$$\{R_{m+n-l}^T\} = \sum_{j=1}^{n_T}\{u^{i_T^j}\}\phi_{m+n-l}^{T,i_T^j}, \qquad \{R_{m+n-l}^q\} = \sum_{j=1}^{n_q}\{u^{i_q^j}\}\phi_{m+n-l}^{q,i_q^j}$$

$$\{R_{m+n-l}^c\} = \sum_{j=1}^{n_c}\{u^{i_c^j}\}\phi_{m+n-l}^{c,i_c^j}$$

Here $\lfloor u^i \rfloor$ is a unit row vector with a unit at i component; the value of i is the grid number of the measured grid. $\{u^{i_T^j}\}$, $\{u^{i_q^j}\}$, and $\{u^{i_c^j}\}$ are the unit column vectors with a unit at i_T^jth, i_q^jth, and i_c^jth component, respectively. Here, the values of ϕ_{m+n-l}^{T,i_T^j}, ϕ_{m+n-l}^{q,i_q^j}, and ϕ_{m+n-l}^{c,i_c^j} are denoted as the unknown boundaries of the temperature condition, the heat flux condition, and the convection condition, respectively. i_T^j, i_q^j, and i_c^j are the grid number of the locations of the estimated function ϕ_{m+n-l}^{T,i_T^j}, ϕ_{m+n-l}^{q,i_q^j}, and ϕ_{m+n-l}^{c,i_c^j}, respectively. The values of n_T, n_q, and n_c are the number of the unknown boundary conditions with respect to the unknown functions ϕ_{m+n-l}^{T,i_T^j}, ϕ_{m+n-l}^{q,i_q^j}, and ϕ_{m+n-l}^{c,i_c^j}, respectively.

Then, the temperatures at i-spatial grid at $(m + n)$ temporal grid can be expressed as follows:

$$\begin{aligned}T_{m+n}^i &= \alpha_{m+n}^i + \beta_{m+n}^i + \sum_{l=0}^{n}\sum_{j=1}^{n_T}\gamma_{m+n,m+l}^{i,i_T^j}\phi_{m+n-l}^{T,i_T^j} \\ &\quad + \sum_{l=0}^{n}\sum_{j=1}^{n_q}\gamma_{m+n,m+l}^{i,i_q^j}\phi_{m+n-l}^{q,i_q^j} + \sum_{l=0}^{n}\sum_{j=1}^{n_c}\gamma_{m+n,m+l}^{i,i_c^j}\phi_{m+n-l}^{c,i_c^j}\end{aligned} \tag{13}$$

where

$$\alpha^i_{m+n} = \lfloor u^i \rfloor [C]^{n+1}\{T_{m-1}\}$$

$$\beta^i_{m+n} = \sum_{l=0}^{n} \lfloor u^i \rfloor [C]^l [D]\{R^0_{m+n-l}\}$$

$$\gamma^{i,i^j_T}_{m+n,m+l} = \lfloor u^i \rfloor [C]^l [D]\{u^{i^j_T}\}$$

$$\gamma^{i,i^j_q}_{m+n,m+l} = \lfloor u^i \rfloor [C]^l [D]\{u^{i^j_q}\}$$

$$\gamma^{i,i^j_c}_{m+n,m+l} = \lfloor u^i \rfloor [C]^l [D]\{u^{i^j_c}\}$$

We substitute the value of n from 0 to $r-1$ into Eq. (13)

$$T^i_m = \alpha^i_m + \beta^i_m + \sum_{j=1}^{n_T} \gamma^{i,i^j_T}_{m,m} \phi^{T,i^j_T}_m + \sum_{j=1}^{q} \gamma^{i,i^j_q}_{m,m} \phi^{q,i^j_q}_m + \sum_{j=1}^{n_c} \gamma^{i,i^j_c}_{m,m} \phi^{c,i^j_c}_m$$

$$T^i_{m+1} = \alpha^i_{m+1} + \beta^i_{m+1} + \sum_{j=1}^{n_T} (\gamma^{i,i^j_T}_{m+1,m} \phi^{T,i^j_T}_{m+1} + \gamma^{i,i^j_T}_{m+1,m+1} \phi^{T,i^j_T}_m)$$
$$+ \sum_{j=1}^{n_q} (\gamma^{i,i^j_q}_{m+1,m} \phi^{q,i^j_q}_{m+1} + \gamma^{i,i^j_q}_{m+1,m+1} \phi^{q,i^j_q}_m)$$
$$+ \sum_{j=1}^{n_c} (\gamma^{i,i^j_c}_{m+1,m} \phi^{c,i^j_c}_{m+1} + \gamma^{i,i^j_c}_{m+1,m+1} \phi^{c,i^j_c}_m)$$

$$T^i_{m+2} = \alpha^i_{m+2} + \beta^i_{m+2}$$
$$+ \sum_{j=1}^{n_T} (\gamma^{i,i^j_T}_{m+2,m} \phi^{T,i^j_T}_{m+2} + \gamma^{i,i^j_T}_{m+2,m+1} \phi^{T,i^j_T}_{m+1} + \gamma^{i,i^j_T}_{m+2,m+2} \phi^{T,i^j_T}_m)$$
$$+ \sum_{j=1}^{n_q} (\gamma^{i,i^j_q}_{m+2,m} \phi^{q,i^j_q}_{m+2} + \gamma^{i,i^j_q}_{m+2,m+1} \phi^{q,i^j_q}_{m+1} + \gamma^{i,i^j_q}_{m+2,m+2} \phi^{q,i^j_q}_m)$$
$$+ \sum_{j=1}^{n_c} (\gamma^{i,i^j_c}_{m+2,m} \phi^{c,i^j_c}_{m+2} + \gamma^{i,i^j_c}_{m+2,m+1} \phi^{c,i^j_c}_{m+1} + \gamma^{i,i^j_c}_{m+2,m+2} \phi^{c,i^j_c}_m)$$

$$T^i_{m+r-1} = \alpha^i_{m+r-1} + \beta^i_{m+r-1}$$
$$+ \sum_{j=1}^{n_T} \gamma^{i,i^j_T}_{m+r-1,m+r-1} \phi^{T,i^j_T}_m + \gamma^{i,i^j_T}_{m+r-1,m+r-2} \phi^{T,i^j_T}_{m+1}$$
$$+ \gamma^{i,i^j_T}_{m+r-1,m+r-3} \phi^{T,i^j_T}_{m+2} + \cdots + \gamma^{i,i^j_T}_{m+r-1,m} \phi^{T,i^j_T}_{m+r-1}$$
$$+ \sum_{j=1}^{n_q} \gamma^{i,i^j_q}_{m+r-1,m+r-1} \phi^{q,i^j_q}_m + \gamma^{i,i^j_q}_{m+r-1,m+r-2} \phi^{q,i^j_q}_{m+1}$$
$$+ \gamma^{i,i^j_q}_{m+r-1,m+r-3} \phi^{q,i^j_q}_{m+2} + \cdots + \gamma^{i,i^j_q}_{m+r-1,m} \phi^{q,i^j_q}_{m+r-1}$$
$$+ \sum_{j=1}^{n_c} \gamma^{i,i^j_c}_{m+r-1,m+r-1} \phi^{c,i^j_c}_m + \gamma^{i,i^j_c}_{m+r-1,m+r-2} \phi^{c,i^j_c}_{m+1}$$
$$+ \gamma^{i,i^j_c}_{m+r-1,m+r-3} \phi^{c,i^j_c}_{m+2} + \cdots + \gamma^{i,i^j_c}_{m+r-1,m} \phi^{c,i^j_c}_{m+r-1} \quad (14)$$

From the preceding derivation, we have

$$\gamma^{i,i^j_T}_{m,m} = \gamma^{i,i^j_T}_{m+1,m} = \cdots = \gamma^{i,i^j_T}_{m+r-1,m} = e^{i,i^j_T}_0$$
$$\gamma^{i,i^j_T}_{m+1,m+1} = \gamma^{i,i^j_T}_{m+2,m+1} = \cdots = \gamma^{i,i^j_T}_{m+r-1,m+1} = e^{i,i^j_T}_1$$
$$\gamma^{i,i^j_T}_{m+n,m+n} = \gamma^{i,i^j_T}_{m+n+1,m+n} = \cdots = \gamma^{i,i^j_T}_{m+r-1,m+n} = e^{i,i^j_T}_n$$

then

$$\gamma^{i,i^j_T}_{m+r-1,m+r-1} = e^{i,i^j_T}_{r-1}$$
$$\gamma^{i,i^j_q}_{m,m} = \gamma^{i,i^j_q}_{m+1,m} = \cdots = \gamma^{i,i^j_q}_{m+r-1,m} = e^{i,i^j_q}_0$$
$$\gamma^{i,i^j_q}_{m+1,m+1} = \gamma^{i,i^j_q}_{m+2,m+1} = \cdots = \gamma^{i,i^j_q}_{m+r-1,m+1} = e^{i,i^j_q}_1$$
$$\gamma^{i,i^j_q}_{m+n,m+n} = \gamma^{i,i^j_q}_{m+n+1,m+n} = \cdots = \gamma^{i,i^j_q}_{m+r-1,m+n} = e^{i,i^j_q}_n$$

then

$$\gamma^{i,i^j_q}_{m+r-1,m+r-1} = e^{i,i^j_q}_{r-1}$$
$$\gamma^{i,i^j_c}_{m,m} = \gamma^{i,i^j_c}_{m+1,m} = \cdots = \gamma^{i,i^j_c}_{m+r-1,m} = e^{i,i^j_c}_0$$
$$\gamma^{i,i^j_c}_{m+1,m+1} = \gamma^{i,i^j_c}_{m+2,m+1} = \cdots = \gamma^{i,i^j_c}_{m+r-1,m+1} = e^{i,i^j_c}_1$$
$$\gamma^{i,i^j_c}_{m+n,m+n} = \gamma^{i,i^j_c}_{m+n+1,m+n} = \cdots = \gamma^{i,i^j_c}_{m+r-1,m+n} = e^{i,i^j_c}_n$$

then

$$\gamma^{i,i^j_c}_{m+r-1,m+r-1} = e^{i,i^j_c}_{r-1} \quad (15)$$

Here, the value of the first and the second superscripts of e represent the measured and estimated grids. The value of the subscript of e is the future time step.

The values of $e^{i,i^j_T}_n$, $e^{i,i^j_q}_n$, and $e^{i,i^j_c}_n$ in Eq. (15) depend on the measured location and the estimated location. The values of $e^{i,i^j_T}_n$, $e^{i,i^j_q}_n$, and $e^{i,i^j_c}_n$ count on the step number of future time but not on the time step in the global temporal coordinate. In other words, the values of $e^{i,i^j_T}_n$, $e^{i,i^j_q}_n$, and $e^{i,i^j_c}_n$ are constants in each evaluation step and they only need to be calculated once when the locations of the measured points and the input boundaries are fixed. On the other hand, the coefficients in Eq. (14) α^i_{m+n} and β^i_{m+n} are derived from the previous state $\{T_{m-1}\}$ and the present known boundary $\{R^0_{m+n-l}\}$. Therefore, these coefficients need to be evaluated at successive time steps.

When $t = t_m$, the estimated condition between $t = t_1$ and $t = t_{m-1}$ has been evaluated and the problem is to estimate the strength of the boundary conditions at $t = t_m$. To stabilize the estimated results in the inverse algorithms, the sequential procedure temporally assumes that several future values of the estimation are constant.[5] Then, the unknown conditions at the future time are assumed to be equal, i.e.,

$$\phi^{T,i^j_T}_{m+1} = \phi^{T,i^j_T}_{m+2} = \cdots = \phi^{T,i^j_T}_{m+r-2} = \phi^{T,i^j_T}_{m+r-1} = \phi^{T,i^j_T}_m$$
$$\phi^{q,i^j_q}_{m+1} = \phi^{q,i^j_q}_{m+2} = \cdots = \phi^{q,i^j_q}_{m+r-2} = \phi^{q,i^j_q}_{m+r-1} = \phi^{q,i^j_q}_m \quad (16)$$
$$\phi^{c,i^j_c}_{m+1} = \phi^{c,i^j_c}_{m+2} = \cdots = \phi^{c,i^j_c}_{m+r-2} = \phi^{c,i^j_c}_{m+r-1} = \phi^{c,i^j_c}_m$$

Substituting Eqs. (15) and (16) into Eq. (14), we obtain

$$T^i_m = \alpha^i_m + \beta^i_m + \sum_{j=1}^{n_T} e^{i,i^j_T}_0 \phi^{T,i^j_T}_m + \sum_{j=1}^{n_q} e^{i,i^j_q}_0 \phi^{q,i^j_q}_m + \sum_{j=1}^{n_c} e^{i,i^j_c}_0 \phi^{c,i^j_c}_m$$

$$T^i_{m+1} = \alpha^i_{m+1} + \beta^i_{m+1} + \sum_{j=1}^{n_T} (e^{i,i^j_T}_0 + e^{i,i^j_T}_1) \phi^{T,i^j_T}_m$$
$$+ \sum_{j=1}^{n_q} (e^{i,i^j_q}_0 + e^{i,i^j_q}_1) \phi^{q,i^j_q}_m + \sum_{j=1}^{n_c} (e^{i,i^j_c}_0 + e^{i,i^j_c}_1) \phi^{c,i^j_c}_m$$

$$T^i_{m+2} = \alpha^i_{m+2} + \beta^i_{m+2} + \sum_{j=1}^{n_T} (e^{i,i^j_T}_0 + e^{i,i^j_T}_1 + e^{i,i^j_T}_2) \phi^{T,i^j_T}_m$$
$$+ \sum_{j=1}^{n_q} (e^{i,i^j_q}_0 + e^{i,i^j_q}_1 + e^{i,i^j_q}_2) \phi^{q,i^j_q}_m + \sum_{j=1}^{n_c} (e^{i,i^j_c}_0 + e^{i,i^j_c}_1 + e^{i,i^j_c}_2) \phi^{c,i^j_c}_m$$

$$T^i_{m+r-1} = \alpha^i_{m+r-1} + \beta^i_{m+r-1}$$
$$+ \sum_{j=1}^{n_T} (e^{i,i^j_T}_0 + e^{i,i^j_T}_1 + e^{i,i^j_T}_2 + \cdots + e^{i,i^j_T}_{r-1}) \phi^{T,i^j_T}_m$$
$$+ \sum_{j=1}^{n_q} (e^{i,i^j_q}_0 + e^{i,i^j_q}_1 + e^{i,i^j_q}_2 + \cdots + e^{i,i^j_q}_{r-1}) \phi^{q,i^j_q}_m$$
$$+ \sum_{j=1}^{n_c} (e^{i,i^j_c}_0 + e^{i,i^j_c}_1 + e^{i,i^j_c}_2 + \cdots + e^{i,i^j_c}_{r-1}) \phi^{c,i^j_c}_m \quad (17)$$

We define

$$T^i_{m+k} = \alpha^i_{m+k} + \beta^i_{m+k} + \sum_{j=1}^{n_T} (e_0^{i,i_T^j} + e_1^{i,i_T^j} + e_2^{i,i_T^j} + \cdots + e_k^{i,i_T^j})\phi_m^{T,i_T^j} + \sum_{j=1}^{n_q} (e_0^{i,i_q^j} + e_1^{i,i_q^j} + e_2^{i,i_q^j} + \cdots + e_k^{i,i_q^j})\phi_m^{q,i_q^j} + \sum_{j=1}^{n_c} (e_0^{i,i_c^j} + e_1^{i,i_c^j} + e_2^{i,i_c^j} + \cdots + e_k^{i,i_c^j})\phi_m^{c,i_c^j} \quad (18)$$

or

$$T^i_{m+k} = \alpha^i_{m+k} + \beta^i_{m+k} + \sum_{j=1}^{n_T} E_k^{i,i_T^j}\phi_m^{T,i_T^j} + \sum_{j=1}^{n_q} E_k^{i,i_q^j}\phi_m^{q,i_q^j} + \sum_{j=1}^{n_c} E_k^{i,i_c^j}\phi_m^{c,i_c^j} \quad (19)$$

where $E_k^{i,i_T^j} = \sum_{l=0}^{k} e_l^{i,i_T^j}$, $E_k^{i,i_q^j} = \sum_{l=0}^{k} e_l^{i,i_q^j}$, $E_k^{i,i_c^j} = \sum_{l=0}^{k} e_l^{i,i_c^j}$, and $k = 0, 1, 2, \ldots, r-1$.

Therefore, Eq. (19) can be expressed as the following form:

$$\boldsymbol{\theta} = \boldsymbol{\Omega}\boldsymbol{\Phi} \quad (20)$$

where

$$\boldsymbol{\Phi} = \begin{Bmatrix} \phi_m^{T,i_T^1} \\ \phi_m^{T,i_T^2} \\ \vdots \\ \phi_m^{T,i_T^{n_T}} \\ \phi_m^{q,i_q^1} \\ \phi_m^{q,i_q^2} \\ \vdots \\ \phi_m^{q,i_q^{n_q}} \\ \phi_m^{c,i_c^1} \\ \phi_m^{c,i_c^2} \\ \vdots \\ \phi_m^{c,i_c^{n_c}} \end{Bmatrix}_{(n_T+n_q+n_c)\times 1}, \quad \boldsymbol{\theta} = \begin{Bmatrix} T_m^{i_1} - \alpha_m^{i_1} - \beta_m^{i_1} \\ T_{m+1}^{i_1} - \alpha_{m+1}^{i_1} - \beta_{m+1}^{i_1} \\ \vdots \\ T_{m+r-1}^{i_1} - \alpha_{m+r-1}^{i_1} - \beta_{m+r-1}^{i_1} \\ T_m^{i_2} - \alpha_m^{i_2} - \beta_m^{i_2} \\ T_{m+1}^{i_2} - \alpha_{m+1}^{i_2} - \beta_{m+1}^{i_2} \\ \vdots \\ T_{m+r-1}^{i_2} - \alpha_{m+r-1}^{i_2} - \beta_{m+r-1}^{i_2} \\ \vdots\vdots\vdots \\ T_m^{i_p} - \alpha_m^{i_p} - \beta_m^{i_p} \\ T_{m+1}^{i_p} - \alpha_{m+1}^{i_p} - \beta_{m+1}^{i_p} \\ \vdots \\ T_{m+r-1}^{i_p} - \alpha_{m+r-1}^{i_p} - \beta_{m+r-1}^{i_p} \end{Bmatrix}_{(p\times r)\times 1}$$

where p is an integer and is denoted as the total number of the measured points.

After the measured temperature Y_j^i (measured at $t = t_j$ and $x = x_i$) is substituted into vector $\boldsymbol{\theta}$, the components of vector $\boldsymbol{\Phi}$ can be found through a linear least-squares error method.[24] Therefore, the result is

$$\hat{\boldsymbol{\Phi}} = (\boldsymbol{\Omega}^T\boldsymbol{\Omega})^{-1}\boldsymbol{\Omega}^T\boldsymbol{\theta} \quad (21)$$

Therefore, the unknown boundary condition $\{R_m^T\}$, $\{R_m^q\}$, and $\{R_m^c\}$ can be solved at successive time steps along with the temporal coordinate. In other words, Eq. (21) provides a sequential algorithm that can be used to estimate the boundary conditions through increasing the value of m by one for each time step because the estimated conditions depend on the measured temperature, the known boundary condition $\{R_m^0\}$, and the previous state $\{T_{m-1}\}$. Moreover, the proposed method is based on the finite element difference approach, and it can be extended to use other kinds of numerical methods through the proposed procedure.

Computational Algorithm

The procedure for the proposed method can be summarized as follows: First, we choose r, the mesh configuration of the problem domain, the temporal size Δt, the measured grids, i.e., $i_1, i_2, \ldots, i_p$, and the estimated grids, i.e., $i_T^1, i_T^2, \ldots, i_T^{n_T}, i_q^1, i_q^2, \ldots, i_q^{n_q}$, and $i_c^1, i_c^2, \ldots, i_c^{n_c}$. Then, matrix $[B]$ and stiffness matrix $[K]$ of the finite element model are known. Thus, matrices $[C]$, $[C]^2, \ldots, [C]^r$ and $[D]$, $[C][D], \ldots, [C]^{r-1}[D]$ can be calculated in advance, and the values of E_k^{i,i_T^j}, E_k^{i,i_q^j}, and E_k^{i,i_c^j} are known before the calculation at each time step. After that, the computing process includes the following steps:

Step 1: Let $j = m$ and the temperature distribution at $\{T_{j-1}\}$ is known.

Step 2: Calculate $\alpha_j^{i_1}, \alpha_{j+1}^{i_1}, \ldots, \alpha_{j+r-1}^{i_1}, \alpha_j^{i_2}, \alpha_{j+1}^{i_2}, \ldots, \alpha_{j+r-1}^{i_2}, \ldots, \alpha_j^{i_p}, \alpha_{j+1}^{i_p}, \ldots, \alpha_{j+r-1}^{i_p}$ and $\beta_j^{i_1}, \beta_{j+1}^{i_1}, \ldots, \beta_{j+r-1}^{i_1}, \beta_j^{i_2}, \beta_{j+1}^{i_2}, \ldots, \beta_{j+r-1}^{i_2}, \ldots, \beta_j^{i_p}, \beta_{j+1}^{i_p}, \ldots, \beta_{j+r-1}^{i_p}$.

Step 3: Collect the measurement $Y_j^{i_1}, Y_{j+1}^{i_1}, \ldots, Y_{j+r-1}^{i_1}, Y_j^{i_2}, Y_{j+1}^{i_2}, \ldots, Y_{j+r-1}^{i_2}, \ldots, Y_j^{i_p}, Y_{j+1}^{i_p}, \ldots, Y_{j+r-1}^{i_p}$.

Step 4: Calculate $\hat{\boldsymbol{\Phi}} = \lfloor \hat{\phi}_j^{T,i_T^1} \; \hat{\phi}_j^{T,i_T^2} \cdots \hat{\phi}_j^{T,i_T^{n_T}} \; \hat{\phi}_j^{q,i_q^1} \; \hat{\phi}_j^{q,i_q^2} \cdots \hat{\phi}_j^{q,i_q^{n_q}} \; \hat{\phi}_j^{c,i_c^1} \; \hat{\phi}_j^{c,i_c^2} \cdots \hat{\phi}_j^{c,i_c^{n_c}} \rfloor^T$ according to Eq. (21).

Step 5: Calculate $\{T_j\}$.

Step 6: Terminate the process if the final time step is attached. Otherwise, let $j = m + 1$ return to step 2.

Results and Discussion

In this section problems defined from Eqs. (1–5) are used as examples to estimate the unknown boundary conditions.

$$\boldsymbol{\Omega} = \begin{bmatrix} E_0^{i_1,i_T^1} & E_0^{i_1,i_T^2} & \cdots & E_0^{i_1,i_T^{n_T}} & E_0^{i_1,i_q^1} & E_0^{i_1,i_q^2} & \cdots & E_0^{i_1,i_q^{n_q}} & E_0^{i_1,i_c^1} & E_0^{i_1,i_c^2} & \cdots & E_0^{i_1,i_c^{n_c}} \\ E_1^{i_1,i_T^1} & E_1^{i_1,i_T^2} & \cdots & E_1^{i_1,i_T^{n_T}} & E_1^{i_1,i_q^1} & E_1^{i_1,i_q^2} & \cdots & E_1^{i_1,i_q^{n_q}} & E_1^{i_1,i_c^1} & E_1^{i_1,i_c^2} & \cdots & E_1^{i_1,i_c^{n_c}} \\ \vdots & \vdots & \vdots & \vdots & \vdots & \vdots & \vdots & \vdots & \vdots & \vdots & \vdots & \vdots \\ E_{r-1}^{i_1,i_T^1} & E_{r-1}^{i_1,i_T^2} & \cdots & E_{r-1}^{i_1,i_T^{n_T}} & E_{r-1}^{i_1,i_q^1} & E_{r-1}^{i_1,i_q^2} & \cdots & E_{r-1}^{i_1,i_q^{n_q}} & E_{r-1}^{i_1,i_c^1} & E_{r-1}^{i_1,i_c^2} & \cdots & E_{r-1}^{i_1,i_c^{n_c}} \\ E_0^{i_2,i_T^1} & E_0^{i_2,i_T^2} & \cdots & E_0^{i_2,i_T^{n_T}} & E_0^{i_2,i_q^1} & E_0^{i_2,i_q^2} & \cdots & E_0^{i_2,i_q^{n_q}} & E_0^{i_2,i_c^1} & E_0^{i_2,i_c^2} & \cdots & E_0^{i_2,i_c^{n_c}} \\ E_1^{i_2,i_T^1} & E_1^{i_2,i_T^2} & \cdots & E_1^{i_2,i_T^{n_T}} & E_1^{i_2,i_q^1} & E_1^{i_2,i_q^2} & \cdots & E_1^{i_2,i_q^{n_q}} & E_1^{i_2,i_c^1} & E_1^{i_2,i_c^2} & \cdots & E_1^{i_2,i_c^{n_c}} \\ \vdots & \vdots & \vdots & \vdots & \vdots & \vdots & \vdots & \vdots & \vdots & \vdots & \vdots & \vdots \\ E_{r-1}^{i_2,i_T^1} & E_{r-1}^{i_2,i_T^2} & \cdots & E_{r-1}^{i_2,i_T^{n_T}} & E_{r-1}^{i_2,i_q^1} & E_{r-1}^{i_2,i_q^2} & \cdots & E_{r-1}^{i_2,i_q^{n_q}} & E_{r-1}^{i_2,i_c^1} & E_{r-1}^{i_2,i_c^2} & \cdots & E_{r-1}^{i_2,i_c^{n_c}} \\ \vdots\vdots\vdots & \vdots\vdots\vdots & \vdots\vdots\vdots & \vdots\vdots\vdots & \vdots\vdots\vdots & \vdots\vdots\vdots & \vdots\vdots\vdots & \vdots\vdots\vdots & \vdots\vdots\vdots & \vdots\vdots\vdots & \vdots\vdots\vdots & \vdots\vdots\vdots \\ E_0^{i_p,i_T^1} & E_0^{i_p,i_T^2} & \cdots & E_0^{i_p,i_T^{n_T}} & E_0^{i_p,i_q^1} & E_0^{i_p,i_q^2} & \cdots & E_0^{i_p,i_q^{n_q}} & E_0^{i_p,i_c^1} & E_0^{i_p,i_c^2} & \cdots & E_0^{i_p,i_c^{n_c}} \\ E_1^{i_p,i_T^1} & E_1^{i_p,i_T^2} & \cdots & E_1^{i_p,i_T^{n_T}} & E_1^{i_p,i_q^1} & E_1^{i_p,i_q^2} & \cdots & E_1^{i_p,i_q^{n_q}} & E_1^{i_p,i_c^1} & E_1^{i_p,i_c^2} & \cdots & E_1^{i_p,i_c^{n_c}} \\ \vdots & \vdots & \vdots & \vdots & \vdots & \vdots & \vdots & \vdots & \vdots & \vdots & \vdots & \vdots \\ E_{r-1}^{i_p,i_T^1} & E_{r-1}^{i_p,i_T^2} & \cdots & E_{r-1}^{i_p,i_T^{n_T}} & E_{r-1}^{i_p,i_q^1} & E_{r-1}^{i_p,i_q^2} & \cdots & E_{r-1}^{i_p,i_q^{n_q}} & E_{r-1}^{i_p,i_c^1} & E_{r-1}^{i_p,i_c^2} & \cdots & E_{r-1}^{i_p,i_c^{n_c}} \end{bmatrix}_{(p\times r)\times(n_T+n_q+n_c)}$$

Two examples are used to demonstrate the proposed method that can estimate the boundary conditions accurately. In example 1, a heated fluid passes through a long pipe that has a cross section with a circular inner surface and a square outer surface. The measured temperature in example 1 is calculated from Eq. (1–5) when the fluid temperature is preselected. Three kinds of boundaries, i.e., the temperature of the fluid, the quantity of the heat flux entering the inner surface, and the temperature in the inner surface, are estimated from the temperature measured from the outer surface of the pipe. In example 2, a rectangular slab is insulated at all sides except the top side. Three cases are discussed in this example. The measured temperatures in the first two cases are calculated when three heat flux pulses with the triangular time history are applied to the top surface of the slab. In the first case, three heat fluxes are assumed to be applied at the top surface of the slab and they are estimated from the measured temperature at the bottom surface of the slab. The results are compared to the solutions of Woodbury and Thakur's approach.[25] In the second case, a mix-typed boundary, i.e., the temperature condition, the flux condition, and the convection condition, is applied at the top surface of the slab and the mix-typed boundary is estimated based on the same measured temperature as case one. In the third case, the desired temperature history at the sensors' locations is preselected and the inverse problem is to choose the proper input heat flux pulses to generate the desired temperature distribution at the preselected locations.

The simulated temperature is generated from the exact temperature in each problem and it is presumed to have measurement errors. In other words, the random errors of measurement are added to the exact temperature. It can be shown in the following equation:

$$T_{i,j}^{\text{meas}} = T_{i,j}^{\text{exact}} + \lambda_{i,j}\sigma \tag{22}$$

where the subscripts i and j are the grid number of spatial-coordinate and temporal-coordinate respectively. $T_{i,j}^{\text{exact}}$ in Eq. (22) is the exact temperature, $T_{i,j}^{\text{meas}}$ is the measured temperature, σ is the standard deviation of measurement errors, and $\lambda_{i,j}$ is a random number. The value of $\lambda_{i,j}$ is calculated by the International Mathematical and Statistical Library subroutine DRNNOR,[26] and chosen over the range $-2.576 < \lambda_{i,j} < 2.576$, which represents the 99% confidence bound for the measurement temperature.

Example 1: Consider a long pipe with the cross section as shown in Fig. 2. The values of the thermal conductivity and the heat capacity per unit volume are $k = 1.5$ W/m °C and $\rho C = 0.15$ J/m^3 °C, respectively. The adiabatic condition is applied at the outer surface. It is initially at a uniform temperature $T_0 = 20$°C, and then suddenly a fluid with a time-varying temperature function $T_f(t)$ ($h = 50$ W/m^2 °C) is applied to the inner surface. The temperature function $T_f(t)$ is a triangular function with time variables and can be expressed by the following forms: $T_f(t) = 20 + 100t$, when $0 < t \leq 1.0$ s; and $T_f(t) = 220 - 100t$, when $1.0 < t \leq 2.0$ s.

The temporal domain is from 0.02 to 2 s, with 0.02-s increments for the example. One thermocouple is located at the outer surface of the pipe and is shown in Fig. 2. A finite element model with 153 nodes and 256 elements is shown in Fig. 3, where symmetry about horizontal and vertical axis is used. The outer boundaries along with the lines of the symmetry are

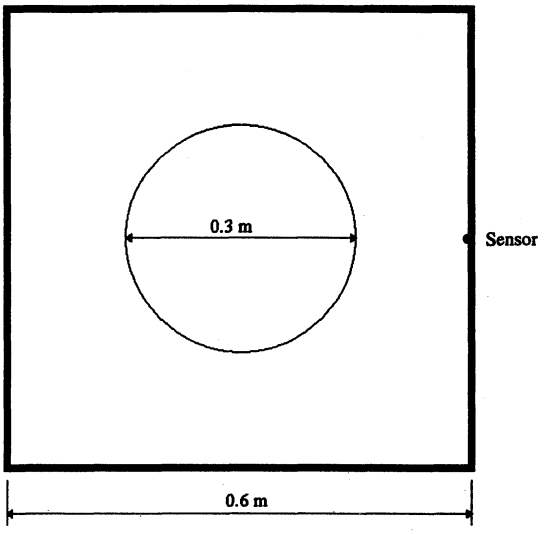

Fig. 2 Cross section of a long pipe in example 1.

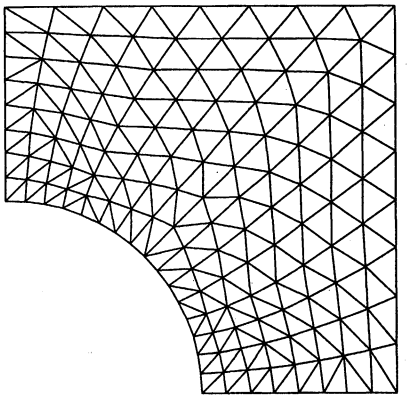

Fig. 3 Mesh configuration with 153 nodes and 256 elements for a quarter of the cross section in example 1.

Table 1 Relative average errors of example 1

Boundary type	$\sigma = 1$	$\sigma = 2$	$\sigma = 3$	$\sigma = 4$	$\sigma = 5$
			$r = 1$		
$T_f(t)$[a]	0.0183103	0.0366202	0.0549304	0.0732405	0.0915506
$q_0(t)$[b]	0.572224	1.14445	1.71667	2.2889	2.86112
$T_b(t)$[c]	0.0163671	0.0327343	0.0491014	0.0654686	0.0818357
			$r = 2$		
$T_f(t)$[a]	0.0161656	0.024767	0.0350491	0.0458406	0.0567729
$q_0(t)$[b]	0.183193	0.361092	0.538992	0.716892	0.894791
$T_b(t)$[c]	0.0163269	0.0240779	0.0339474	0.0442764	0.0547265
			$r = 4$		
$T_f(t)$[a]	0.0467445	0.0454533	0.0455837	0.0484361	0.052402
$q_0(t)$[b]	0.103026	0.167819	0.232642	0.297465	0.362287
$T_b(t)$[c]	0.0482717	0.0468967	0.0466952	0.0491658	0.0529662

[a]Convection boundary. [b]Heat flux boundary. [c]Temperature boundary.

insulated because no heat can flow across them. Three types of boundary conditions are discussed in this example. First, the convection temperature $T_f(t)$ is estimated when the temperature history is available in the sensor location. The heat flux $q_0(t)$ entering the inner surface and the temperature $T_b(t)$ along with the inner surface are then estimated separately according to the temperature measurement at the sensor location.

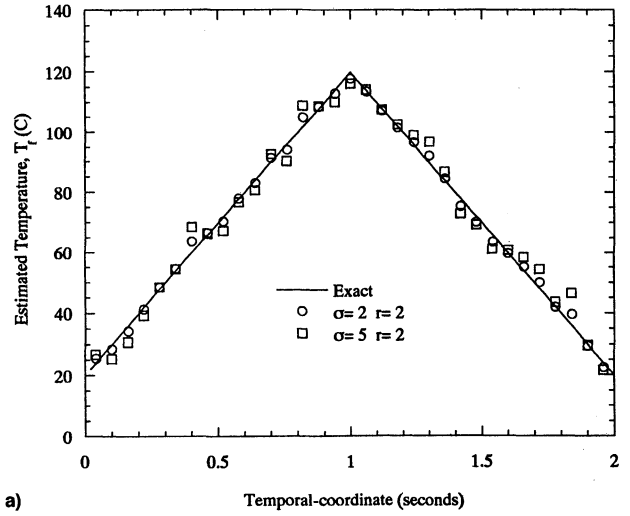

a)

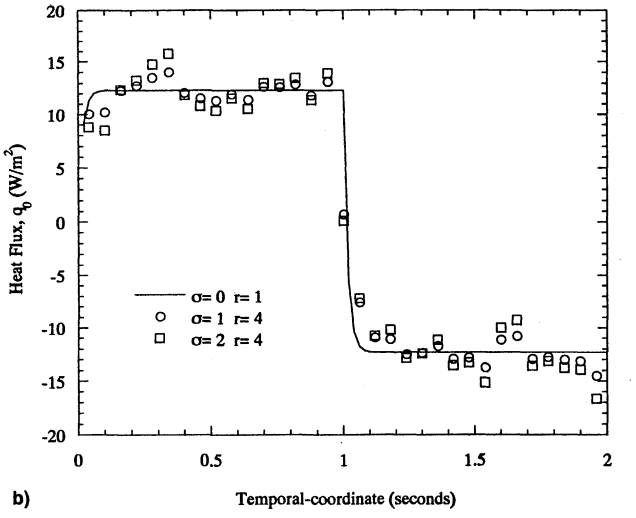

b)

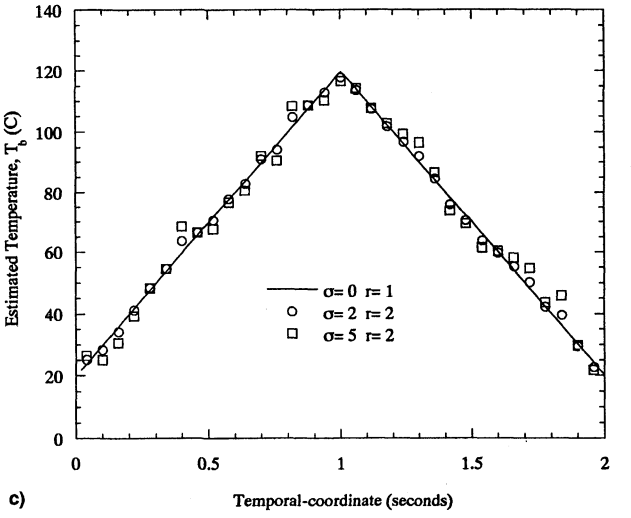

c)

Fig. 4 Estimation of a) the convection temperature pass through the inner surface in example 1, b) the heat flux in the inner surface in example 1, and c) the temperature along the inner surface in example 1.

To investigate the deviation of the estimated results from the error-free solution, the relative average errors for the estimated solutions are defined as follows:

$$\varepsilon = \frac{1}{n_t}\sum_{j=1}^{n_t}\left|\frac{f - f_0}{f_0}\right| \tag{23}$$

where f is the estimated result with measurement errors, f_0 is the estimated result without measurement errors, and n_t is the number of the temporal steps. It is clear that a smaller value of ε indicates a better estimation and vice versa.

When measurement errors are considered, the relative average errors of the estimated results are shown (Table 1), whereas r = 1, 2, and 4. The results show that the heat flux estimation is less accurate than those of the temperature estimation in the temperature boundary or in the convection boundary. In other words, the heat flux estimation is more sensitive to the measurement error than the temperature estimation. For example, when $\sigma = 1$ and $r = 4$, the value of ε is 0.103026 in the heat flux estimation, but 0.0467445 in the convection condition estimation and 0.0482717 in the temperature condition estimation. It is also interesting to investigate the relationship among the average relative error ε, the standard deviation of measurement errors σ, and the number of the future time r. In the flux condition estimation, it does not matter if the value of σ is one, two, three, four, or five, a better estimation appears when the number of future time increases. However, in the estimations of convection boundary and temperature boundary, when the number of future time increases, the estimated results are not necessarily satisfactory. For example, when $\sigma = 1$ and 2, the best estimation is $r = 2$ and the worst estimation is $r = 4$; when $\sigma = 3$ and 4, the best estimation is $r = 2$ and the worst estimation is $r = 1$; when $\sigma = 5$, the best estimation is $r = 4$ and the worst estimation is $r = 1$.

When $\sigma = 0$ and $r = 1$, the estimated results have approximated the exact solution in the convection boundary estimation (Fig. 4a). The estimated result appears as a quarter sinusoidal function and a triangular function in the flux condition estimation and the temperature condition estimation, respectively (Figs. 4b and 4c). It satisfies the physical phenomenon of a pipe with inner fluid that has a uniform temperature with a triangular time-varying form. Furthermore, the estimated results with the measurement error are also shown in Fig. 4. In general, large errors make the estimated results diverge from the error-free solution. For example, the results shown in Fig. 4a have the maximum deviation from their exact solutions when $\sigma = 5$. Moreover, it appears that the results in Figs. 4b and 4c have a similar trend as that in Fig. 4a.

Example 2: Consider a rectangular slab in which all sides, except for the top side, are insulated. The values of the thermal

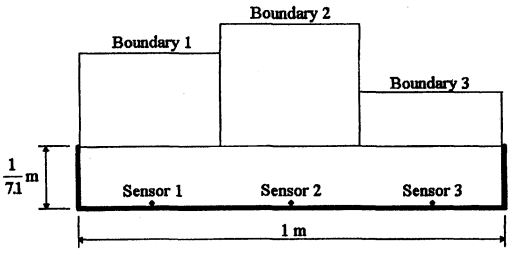

Fig. 5 Boundary conditions, the locations of the sensor, and the dimensions of the slab in example 2.

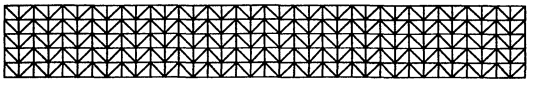

Fig. 6 Mesh configuration with 222 nodes and 360 elements for the rectangular slab in example 2.

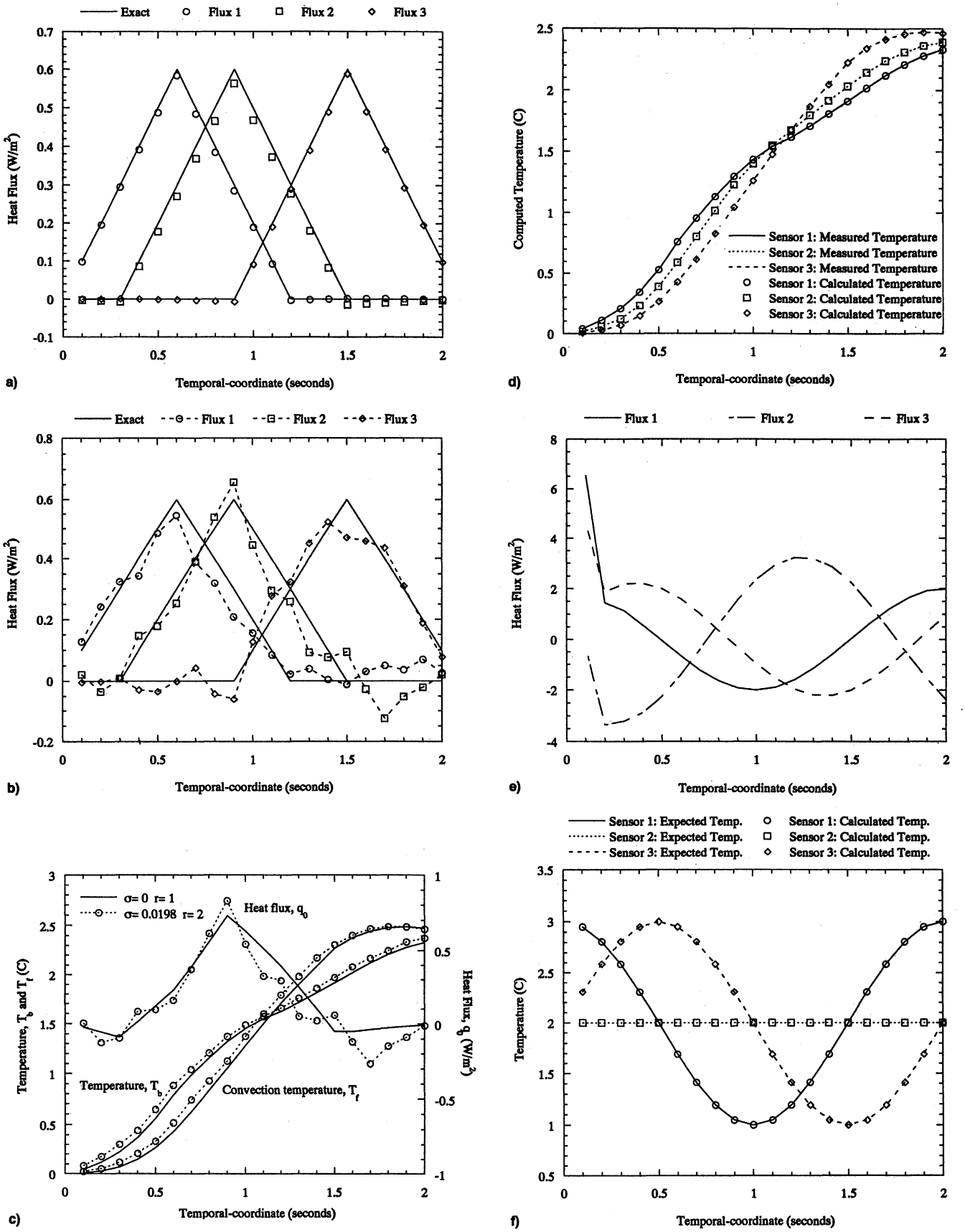

Fig. 7 Estimation of the a) multiflux pulses in example 2 when $\sigma = 0$ and $r = 1$ and b) when $\sigma = 0.0198$ and $r = 2$. c) Estimation of the mix-typed boundary conditions in example 2. d) Comparison of the calculated temperature from the mix-typed boundary conditions with the measured temperature from the multiflux pulses in example 2 when $\sigma = 0$ and $r = 1$. e) Designed flux pulses to generate a sine, constant, and cosine temperature distribution at sensors location in example 2. f) Comparison of the calculated temperature from the designed boundary conditions with the measured temperature from the preselected boundary conditions in example 2 when $\sigma = 0$ and $r = 1$.

conductivity and the heat capacity per unit volume are $k = 1.0$ W/m °C and $\rho C = 0.4$ J/m^3 °C, respectively. The adiabatic conditions are applied to the left, right, and bottom surfaces. It is initially at a uniform temperature $T_0 = 0$°C over the slab, and then three boundary conditions are suddenly applied to the top surface of the slab (Fig. 5).

The temporal domain is from 0.1 to 2 s, with 0.1-s increment for the example. Three thermocouples are located at the bottom surface of the slab (Fig. 5). A finite element model with 222 nodes and 360 elements is constructed and shown in Fig. 6. The measurement temperature errors are set within -0.051 to 0.051, which implies that the average standard deviation of measurements is 0.0198, i.e., $\sigma = 0.0198$, for a 99% confidence bound.

In the first case, three heat fluxes with the triangular time history are assumed to be applied at the top surface of the slab and they are estimated from the measured temperature at the bottom surface of the slab. When measurement errors are not included, the results have good approximations (Fig. 7a). When measurement errors, i.e., $\sigma = 0.0198$, are included the estimated results remain satisfied (see Fig. 7b). The same case has also been done by Woodbury and Thakur,[25] who used a method based on a discrete Duhamel's Theorem and Beck's function specification method. From the results, it appears that the maximum deviation is about 0.5 in their paper, while it is only about 0.15 in the present research. In other words, compared with the research by Woodbury and Thakur (Figs. 6 and 8 in Ref. 25), a more favorable result can be approached through the proposed method in the present research.

To further test the applicability of the proposed method, the same measurements from case 1 are adopted to estimate a problem with mix-typed boundary conditions, i.e., the temperature boundary, the heat flux boundary, and the convection boundary ($h = 50$ W/m^2 °C). The results show that the proposed method is able to estimate the mix-typed boundary conditions (Fig. 7c). To confirm the accuracy of the estimated results, we substitute the results from $\sigma = 0$ and $r = 1$ into the process of the direct analysis. The results show that the direct solution has a good match to the measured temperature (Fig. 7d).

In the last case, the proposed method is used to design a set of input flux to generate an expected temperature history at the desired locations. For illustration, the desired temperature distribution is a sine function at sensor 1, a constant temperature at sensor 2, and a cosine function at sensor 3. The designed heat fluxes are shown in Fig. 7e. The generated temperature field and the expected temperature field are also shown in Fig. 7f. It shows that the temperature field generated from the designed fluxes is in good agreement with the desired temperature field.

All numerical calculations from examples 1 and 2 are performed on a personal computer with a Pentium-133 CPU. When $[C]$ and $[D]$ are available [Eq. (11)], the CPU time needed in example 1 is under 1.04 s when r is equal to 1, 1.95 s when r is equal to 2, and 3.74 s when r is equal to 4. In example 2, the CPU time is under 0.65 s and 4.35 s for $r = 1$ and 2, respectively. Therefore, the proposed method is very fast.

It can be concluded that the proposed method is an accurate, robust, and efficient method to determine the boundary conditions in inverse heat conduction problems.

Conclusions

A sequential method has been introduced for determining the boundary condition in the inverse conduction problems. The inverse solution is represented as a closed form derived from a finite difference element method when the temperature measurements are available. Special features about this method are that no preselect functional form for the unknown function is necessary and no sensitivity analysis is needed in the algorithm. Two examples have been illustrated based on the proposed method. In the first example, the accuracy of the estimated results in the different types of the boundary conditions are investigated. The results show that the heat flux estimation is more sensitive to the measurement error than the temperature estimation. The relationship among the average relative errors, the standard deviation of measurement errors, and the number of the future time steps is also investigated. A larger number of the future time steps is needed to get a more accurate result when measurement error is larger. Furthermore, the estimated results with different measurement errors are also discussed; it indicates that large errors make the estimated results diverge from the error-free solution. In the second example, the accuracy of the estimation is more satisfactory than that in past research. Furthermore, it also shows that the proposed method can treat the problem with the mix-typed boundary and the proposed method can be used to design a set of input flux to generate an expected temperature history at the desired locations. In conclusion, from the results in the examples, it appears that the proposed method is an accurate, robust, and efficient inverse technique. The proposed method is applicable to the other kinds of inverse problems such as source strength estimation in the multidimensional inverse conduction problem.

References

[1]Hadamard, J., *Lectures on the Cauchy Problem in Linear Partial Differential Equations*, Yales Univ. Press, New Haven, CT, 1923.

[2]Cannon, J. R., *Numerical Solutions of Nonlinear Differential Equations*, Wiley, New York, 1966.

[3]Yang, C.-Y., "Solving the Two Dimensional Inverse Heat Source Problem Through the Linear Least-Squares Error Method," *Internation Journal of Heat and Mass Transfer*, Vol. 41, No. 2, 1998, pp. 393–398.

[4]Tikhonov, A. N., and Arsenin, V. Y., *Solutions of Ill-Posed Problems*, 1st ed., Winston, Washington, DC, 1977.

[5]Beck, J. V., Blackwell, B., and Clair, C. R. St., *Inverse Heat Conduction—Ill-Posed Problem*, 1st ed., Wiley, New York, 1985.

[6]Morozov, V. A., and Stessin, M., *Regularization Methods for Ill-Posed Problems*, 1st ed., CRC Press, Boca Raton, FL, 1993.

[7]Alifanov, O. M., *Inverse Heat Transfer Problems*, 1st ed., Springer–Verlag, Berlin, 1994.

[8]Liu, J., "A Stability Analysis on Beck's Procedure for Inverse Heat Conduction Problems," *Journal of Computational Physics*, Vol. 123, No. 1, 1995, pp. 65–73.

[9]Reinhardt, H. J., "Numerical Method for the Solution of the Two-Dimensional Inverse Heat Conduction Problem," *Internation Journal for Numerical Methods in Engineering*, Vol. 32, No. 2, 1991, pp. 363–383.

[10]Alifanov, O. M., and Artyukhin, E. A., "Regularized Numerical Solution of Nonlinear Inverse Heat Conduction Problem," *Journal of Engineering Physics*, Vol. 29, No. 1, 1975, pp. 934–938.

[11]Alifanov, O. M., and Mikhailov, V. V., "Solution of the Nonlinear Inverse Thermal Conductivity Problem by the Iteration Method," *Journal of Engineering Physics*, Vol. 35, No. 6, 1978, pp. 1501–1506.

[12]Beck, J. V., and Murio, D. A., "Combined Function Specification-Regularization Procedure for Solution of Inverse Heat Conduction Problem," *AIAA Journal*, Vol. 24, No. 1986, pp. 180–185.

[13]Busby, H. R., and Trujillo, D. M., "Numerical Solution to a Two-Dimensional Inverse Heat Conduction Problem," *International Journal for Numerical Methods in Engineering*, Vol. 21, 1985, pp. 349–359.

[14]Murio, D. A., *The Mollification Method and the Numerical Solution of Ill-Posed Problems*, Wiley-Interscience, New York, 1993.

[15]Jarny, Y., Ozisik, M. N., and Bardon, J. P., "A General Optimization Method Using Adjoint Equation for Solving Multidimensional Inverse Heat Conduction," *International Journal of Heat and Mass Transfer*, Vol. 34, No. 11, 1991, pp. 2911–2919.

[16]Dorai, G. A., and Tortorelli, D. A.,"Transient Inverse Heat Conduction Problem Via Newton's Method," *International Journal of Heat and Mass Transfer*, Vol. 40, No. 17, 1997, pp. 4115–4127.

[17]Li., H. Y., and Yang, C.-Y., "A Genetic Algorithm for Inverse Radiation Problems," *International Journal of Heat and Mass Transfer*, Vol. 40, No. 7, 1997, pp. 1545–1549.

[18]Yang, C. Y., "Noniterative Solution of Inverse Heat Conduction Problems in One Dimension," *Communcations in Numerical Methods in Engineering*, Vol. 13, 1997, pp. 419–427.
[19]Yang, C.-Y., "Symbolic Computation to Estimate Two-Sided Boundary Conditions in Two-Dimensional Conduction Problems," *Journal of Thermophysics and Heat Transfer*, Vol. 11, No. 3, 1997, pp. 472–476.
[20]Noor, A. K., and Andersen, C. M., "Computerized Symbolic Manipulation in Structural Mechanics of Progress and Potential," *Computers and Structures*, Vol. 10, 1979, pp. 95–118.
[21]Carnahan, B., Luther, H. A., and Wilkes, J. O., *Applied Numerical Methods*, 1st ed., Wiley, New York, 1977.
[22]Celia, M. A., and Gray, W. G., *Numerical Methods for Differential Equations*, Prentice–Hall, Englewood Cliffs, NJ, 1992.
[23]Hsu, T. R., Sun, N. S., Chen, G. G., and Gong, Z. L., "Finite Element Formulation for Two-Dimensional Inverse Heat Conduction Analysis," *Journal of Heat Transfer*, Vol. 114, Aug. 1992, pp. 553–557.
[24]Strang, G., *Linear Algebra and Its Application*, 2nd ed., Academic, New York, 1980.
[25]Woodbury, K. A., and Thakur, S. K., "A Two Dimensional Inverse Heat Conduction Algorithm," *Inverse Problem in Engineering: Theory and Practice*, edited by N. Zabaras, K. Woodbury, and M. Raynaud, American Society of Mechanical Engineers, New York, 1993, pp. 219–226.
[26]*User's Manual: Math Library Version 1.0, IMSL Library Edition 10.0*, International Mathematical and Statistical Library, Houston, TX, 1987.